ARTICLE

Enhancing Shielding of Triplet Energy Transfer to Poly(*p*-phenylene)s from Phosphor Dopant by Addition of Branched Alcohol for Highly Efficient Electrophosphorescence

Yu-Kai Huang, Tzu-Hao Jen, Yao-Tang Chang, Neng-Jye Yang, Hsin-Hung Lu, and Show-An Chen*

Chemical Engineering Department, National Tsing-Hua University, Hsinchu, 30041, Taiwan, R.O.C.

ABSTRACT To obtain an efficient electrophosphorescent device, one needs to consider quenching of phosphor phosphorescence brought by the low triplet energy of the host because the exothermic energy transfer can effectively quench phosphor phosphorescence and markedly lower the device efficiency. Here, a facile approach of adding a branched alcohol (3-*tert*-butyl-2,2,4,4-tetramethylpentan-3-ol, ROH) into green emission phosphor-doped dialkoxyl-substituted poly(para-phenylene)s (PPPs) is demonstrated to effectively enhance shielding of triplet energy transfer to PPPs from the phosphor, resulting from a formation of self-assembly structure that block direct contact between phosphor and the main chains. The green electrophosphorescent device performance can be improved from 7.1 and 32.2 cd/A to 25.1 and 42 cd/A for PPP with dioctoxyl substituents (dC_8OPPP) and with carbozole (Cz)-capped dialkoxyl-substituents (CzPPP), respectively. The latter result 42 cd/A is the highest record for green emission in polymer light emitting diode. This finding suggests that promotion of specific electro-optical properties for small molecule and polymer can be obtained through a self-assembling interaction in addition to chemical structure modification.

KEYWORDS: self-assembly • Dexter energy transfer • shielding effect • electrophosphorescent device • poly(*p*-phenylene)s • electroluminescent polymers

INTRODUCTION

In organic and polymer light-emitting diodes (OLED and PLED), holes and electrons injected from the anode and cathode can recombine to yield singlet excitons (SE) and triplet excitons (TE) at a population ratio of 1:3 according to quantum statistics, which was confirmed for OLED (1), but remains debated for PLED (2, 3). For electrofluorescence devices, only SE is emissive and most energy is wasted by nonemissive TE. However, for electrophosphorescence devices, in which a phosphor (guest) is doped into an organic molecule or polymer host, both SE and TE formed in the host can be harvested by the guest and consequently the internal quantum efficiency is possible to be promoted toward 100% (4). The reason is that the strong spin−orbital coupling in the phsphor can promote its efficiency of intersystem crossing (ISC) from singlet excited state to triplet excited state (5) and radiative decay of its TE (phosphorescence) becomes allowed at room temperature. Therefore, for such host/guest systems, the SE and TE formed in the host under electrical excitation can transfer to phosphor via Förster and Dexter energy transfer, respectively, and SE in phosphor is converted to TE by efficient ISC. Finally, radiative decay of TE (phosphorescence) in the phosphor gives light emission.

In electrophosphorescence devices, TE in the phsphor guest can also be efficiently generated by charge trapping (CT) (6), through which holes and electrons injected from the anode and cathode can directly recombine on the phosphor. In this case, TE formed in the phosphor will finally relax to the ground state accompanied by phosphorescence emission.

To obtain efficient electrophosphorescent device, one needs to consider quenching of phosphor phosphorescence by host triplet. Therefore, a host material with triplet energy (E_T) higher than that of phosphor guest is intuitively required as back triplet energy tranfer (phosphorescence quenching) from high E_T guest to low E_T host can occur, as evidenced by the Stern−Volmer analysis for the system of various phosphors ranging from blue to red emission with tris(9,9-dimethylfluorene) (F3) as the phosphor quencher (7). For high E_T, excellent performance with the maximum luminous efficiency (η_L) about 23 cd/A was obtained for conjugated polymers such as poly(3,6-carbazole) derivatives (P(3,6-Cz)s) with $E_T \approx 2.6$ eV (8, 9) upon being doped with green-emitting Ir complex, bis(2-phenylpyridine)(acetylacetonate)iridium(III) (Ir-G, $E_T = 2.41$ eV). However, for common blue-emitting polymers (10), such as polyfluorenes (PFs) ($E_T = 2.18$ eV) and poly(*p*-phenylene)s (PPPs) ($E_T = 2.27$ eV), their E_T values are usually low and expected to be not suitable for use as hosts for high E_T guests, such as Ir-G. Because triplet energy transfer between conjugated polymer host and phosphor guest is via the Dexter mechanism (requiring a close contact within 15 Å) (11), some efforts (12–14) have been attempted

* To whom correspondence should be addressed. Tel: 886-3-5710733. Fax: 886-3-5737798. E-mail: sachen@che.nthu.edu.tw.
Received for review December 10, 2009 and accepted March 11, 2010

DOI: 10.1021/am900878f

Published on Web 04/09/2010

to reduce the back triplet energy transfer from guest to host by increasing host−guest separation. In our recently work (14), we have demostrated that an effective shielding of triplet energy transfer from the high E_T phosphor, Ir-G, to the low E_T PPPs is possible by introducing dense side chains to the polymer backbone for blocking a direct contact from the guest such that possibility of Dexter energy transfer between them is significantly reduced, as evidenced by the Stern−Volmer analysis and excellent device luminous efficiency (η_L) of 30 cd/A (its corresponding external quantum efficiency η_{ext} is 8.25%), which is more efficient than that (23 cd/A) in the system with high E_T host (8, 9). Alternatively, introducing bulky t-butyl as side group on each ring in the ligands of green-emitting Ir(ppy)$_3$ ($E_T = 2.4$ eV) has also been found to promote the η_{ext} to 0.4% when used as a dopant for poly(9,9′-spirobifluorene) ($E_T = 2.18$ eV) as compared to the system with the same dopant but without such modification ($\eta_{ext} = 0.1$%), which reflects a reduced triplet energy transfer back to the host (13).

From the reviews above, it suggests that the E_T of polymer host is not necessary to be higher than that of phosphor guest for efficient electrophosphorescence and, in addition, phosphorescence quenching can also be effectively reduced or completely prevented by increasing host−guest distance. Here, a facile approach of adding a branched alcohol (3-*tert*-butyl-2,2,4,4-tetramethylpentan-3-ol, ROH) into the emitting layer composed of low E_T PPPs as host and high E_T Ir-G as guest of the electrophosphorescent device is demonstrated to effectively reduce the close contact between host and guest and thus largely reduce quenching of phosphor phosphorescence. The polymer hosts investigated are PPPs with dioctoxyl substituents (dC$_8$OPPP, $E_T = 2.31$ eV) (14) and with carbozole (Cz)-capped dialkoxyl-substituents (CzPPP, $E_T = 2.39$ eV) (14), which have been proven that the alkoxyl side chains in these PPPs can effectively shield the back triplet energy transfer from high E_T phosphor as mentioned above. With the adddition of ROH, the separations between polymers and Ir-G are promoted possibily through hydrogen bonding among them. The efficiencies of corresponding devices can be improved from 7.1 and 32.2 cd/A to 25.1 and 42 cd/A for dC$_8$OPPP/Ir-G and CzPPP/Ir-G, respectively, when an appropriate amount of ROH is added. This finding suggests that a promotion of specific electro-optical property for phosphor-doped polymer system can be obtained through self-assembling interaction in addition to chemical structure modification.

EXPERIMENTAL SECTION

Photoluminescence (PL) and electroluminescence (EL) spectra were measured using a fluorescence spectrometer (Jobin Yvon Horiba, Fluoromax-3). Current−voltage characteristics and luminance of the device were measured using Keithley power supply (model 238) and luminance meter (BM8 from TOPCON), respectively, and both are computer controlled with a Labview program. Fourier transform infrared (FTIR) spectrometer (IFS/66S from Bruker) was used to perform IR measurements and the films used for the measurements were cast on KBr substrates from their solutions in tetrahydrofuran (THF) of polymers, Ir-G, ROH, and blends. The thickness of polymer film was measured by Tencor P-10 Surface Profiler. ^{1}H NMR spectrum was recorded with Varian Unityinova 500 NMR. Mass spectrum (MS) was recorded using a mass spectrometer (HEWLETT PACKARD, 5972 SERIES). The scanning probe microscopy (Digital Instrument Nanoscope V) was performed under ambient atmosphere. Rectangular Au tips (Multi75GB, Budget Sensors) with an estimated force constant of 3 N/m and resonance frequency of 75 kHz were used in tapping mode for topographical images. The surface roughness was obtained by using the affiliated software.

The synthetic procedure for 3-*tert*-butyl-2,2,4,4-tetramethylpentan-3-ol (ROH) is as follows. Under a nitrogen atmosphere, 2,2,4,4-tetramethylpentan-3-one (5 mL, 29 mmol) was dissolved in 60 mL of diethyl ether. The solution was cooled to −78 °C, and then a solution of *tert*-butyllithium in pentane (0.15 vol.%, 26.9 mL, 43.5 mmol) was added dropwise. The reaction mixture was stirred for 4 h at −78 °C under a nitrogen atmosphere. After the reaction mixture was warmed to room temperature, water (100 mL) and then a saturated aqueous solution of ammonium chloride was added until this mixture became neutral (pH ∼7). The mixture was extracted with diethyl ether to collect the organic phase, which was dried over anhydrous magnesium sulfate ($MgSO_4$) and the diethyl ether was removed under a vacuum to give a colorless gel product. (4.76 g, yield 82%). ^{1}H NMR (500 MHz, $CDCl_3$). δ (ppm): 1.38 (s, 1H), 1.26 (s, 27H). MS: $m/z = 200$.

The fabrication procedures for the devices are as follows: indium−tin oxide (ITO) glass was treated with oxygen plasma. For dC$_8$OPPP/Ir-G devices, a thin layer (15 nm) of poly(styrene sulfonic acid)-doped poly(ethylenedioxythiophene) (PEDOT:PSS, Baytron P AI 4083 from Bayer) was spin-coated on the treated ITO; For CzPPP/Ir-G devices, a CFx thin film (15, 16) (2 nm) was coated on treated ITO by plasma polymerization of CF_3H in a chamber of parallel electrode type equipped with a 13.56 MHz radio frequency power generator. PEDOT:PSS or CFx act as a hole injection layer in the devices. On top of the treated ITO glass, an emitting layer (about 90 nm) was spin-coated from its solution in THF. In the case of CzPPP/Ir-G, a layer of 1,3,5-tri(phenyl-2-benzimidazolyl)-benzene (TPBI) (30 nm), which was used as a hole/exciton blocking layer, was grown by thermal evaporation in a vacuum thermal evaporator through a shadow mask at a vacuum of 2×10^{-6} Torr. Finally, a thin layer of CsF (about 1.5 nm) and then calcium (about 1.5 nm) covered with a layer of aluminum as the cathode for the bipolar device were deposited in a vacuum thermal evaporator through a shadow mask at a pressure of less than 2×10^{-6} Torr. The active area of the device is about 13.5 mm^2.

RESULTS AND DISCUSSION

The chemical structures of dC$_8$OPPP, CzPPP, Ir-G, and ROH are shown in Chart 1. The polymers (dC$_8$OPPP and CzPPP) were synthesized according to the procedures in our previous report (14). Ir-G was purchased from Lumtec Technology (Taiwan) and used without further purification. The synthetic route for ROH is given in Scheme 1.

Figure 1a shows the normalized PL spectra of Ir-G doped PPPs thin films (PPPs:Ir-G weight ratio, 1:0.08) with different amounts of ROH (weight ratio relative to dC$_8$OPPP: 0.025−0.75 and weight ratio relative to CzPPP:0.02−0.3). The emission peaks are observed at 405 nm for dC$_8$OPPP and at 400 nm for CzPPP, whereas the peak locates at 518 nm is attributed to Ir-G. Upon adding ROH in the emitting blends, predominant Ir-G emissions are observed with PPPs as hosts, but no host emission for CzPPP and a weak host emission for dC$_8$OPPP. This difference is mainly due to better chemical compatibility in CzPPP/Ir-G than that in

Chart 1. Chemical Structures of dC_8OPPP, CzPPP, Ir-G, and ROH

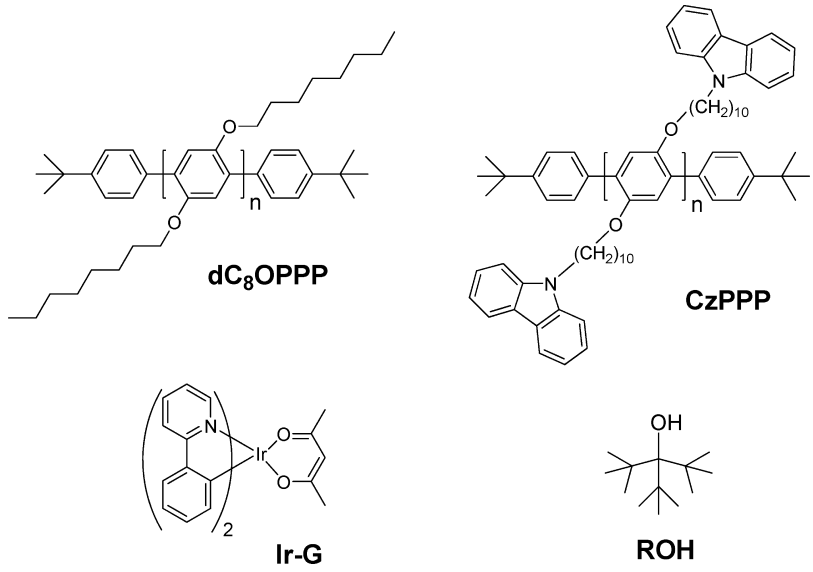

Scheme 1. Synthetic Route for the Branched Alcohol 3-*Tert*-butyl-2,2,4,4-tetramethylpentan-3-ol (ROH)

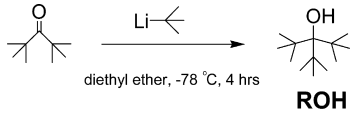

dC_8OPPP/Ir-G (14); therefore, Förster energy transfer is more efficient in CzPPP/Ir-G than that in dC_8OPPP/Ir-G upon photoexcitation. The relative host/guest intensities do not change significantly in both cases when the weight ratios of ROH relative to PPPs increase from 0.02 to 0.3. When the weight ratio of ROH to dC_8OPPP further increases to 0.75, the host emission further increases as compared to that of other ROH loading, which may be ascribed to the excess ROH addition that leads to an increase in host−guest distance and thus results in poor Förster energy transfer efficiency between the host and guest.

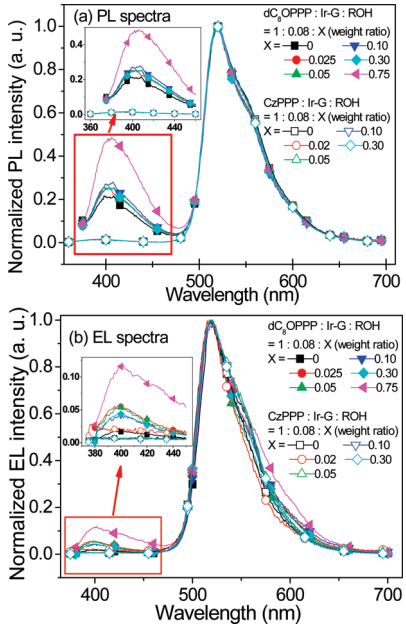

FIGURE 1. Normalized (a) PL (excited at 350 nm) and (b) EL spectra of Ir-G doped PPPs thin films with different amount of ROH. The weight ratios of Ir-G and ROH are relative to host polymer. The emission peaks are 405 and 400 nm for dC_8OPPP and CzPPP, respectively. For Ir-G, the peak maximum locates at 518 nm.

Figure 1b shows the normalized EL spectra of Ir-G doped PPPs thin films with various amounts of ROH. A strong Ir-G emission are observed in both cases, which is due to an occurrence of charge trapping in these systems (14). Weak host emission is observed with dC_8OPPP as a host. The reason is that SE formed in the dC_8OPPP (the SE generated directly in dC_8OPPP is small in population because of the occurrence of charge trapping in dC_8OPPP/Ir-G) can not transfer to Ir-G efficiently due to poor chemical compatibility mentioned above. When the weight ratio of ROH to dC_8OPPP rises to 0.75, the host emission increases, which may be ascribed to an increased host−guest distance due to excess ROH addition, leading to a reduced chance for charge trapping.

Table 1 lists the performances (turn-on voltage, luminous efficiency, and brightness) of the devices for Ir-G doped PPPs with different amount of ROH. As can be seen in Table 1, there is an optimal amount of ROH for achieving green emission with excellent device efficiency. For dC_8OPPP/Ir-G, the best device performance (η_{Lmax} = 25.1 cd/A and B_{max} = 1184 cd/m^2) is observed at the weight ratio of ROH/dC_8OPPP = 0.025, which is more efficient and brighter than that (η_{Lmax} = 7.1 cd/A and B_{max} = 700 cd/m^2) without adding ROH. In the case of CzPPP/Ir-G, addition of ROH at the weight ratio of 0.05 relative to CzPPP gives the best device performance (η_{Lmax} = 42 cd/A and B_{max} = 5685 cd/m^2). This efficiency is the highest recorded among the reported green emission in PLEDs. The corresponding brightness and luminous efficiency versus current density for dC_8OPPP/Ir-G and CzPPP/Ir-G devices with and without ROH addition are shown in Figure 2. The improved maximum device efficiency for dC_8OPPP/Ir-G with the ROH addition as compared to that without ROH addition (from 7.1 to 25.1 cd/A)

Table 1. Device[a] Performances of Ir-G as Guest and dC_8OPPP or CzPPP as Host with Different Amounts of ROH

	Ir-G		ROH				
host	weight ratio[b]	mole ratio[c]	weight ratio[b]	mole ratio[c]	turn-on voltage[d]	η_{Lmax}[e] (cd/A)	B_{max}[e] (cd/m^2)
dC_8OPPP	0.08	0.044	0	0	11	7.1	700
			0.025	0.041	12.5	25.1	1184
			0.05	0.083	15.5	9.4	750
			0.1	0.17	13	7	573
			0.3	0.50	12	5.6	1050
			0.75	1.25	10	2.3	650
CzPPP	0.08	0.096	0	0	7	32.2	5603
			0.02	0.072	6	32.7	6848
			0.05	0.18	7	42	5685
			0.1	0.36	6.5	38.6	3336
			0.3	1.08	9	23.9	2047

[a] The device structure is ITO/PEDOT:PSS (15 nm)/emitting layer (90 nm)/CsF (1.5 nm)/Ca (1.5 nm)/Al (65 nm) with dC_8OPPP as a host. In the case of CzPPP as a host, the device structure is ITO/CFx (2 nm)/emitting later (90 nm)/TPBI (30 nm)/CsF (1.5 nm)/Ca (1.5 nm)/Al (65 nm). [b] The weight ratios of Ir-G and ROH are relative to the host polymer. [c] The mole ratios of Ir-G and ROH are relative to repeat unit of the host polymer. [d] The turn-on voltage was taken at 0.2 cd/m^2. [e] The data for brightness (B_{max}) and luminous efficiency (η_{Lmax}) are the maximum values of the device.

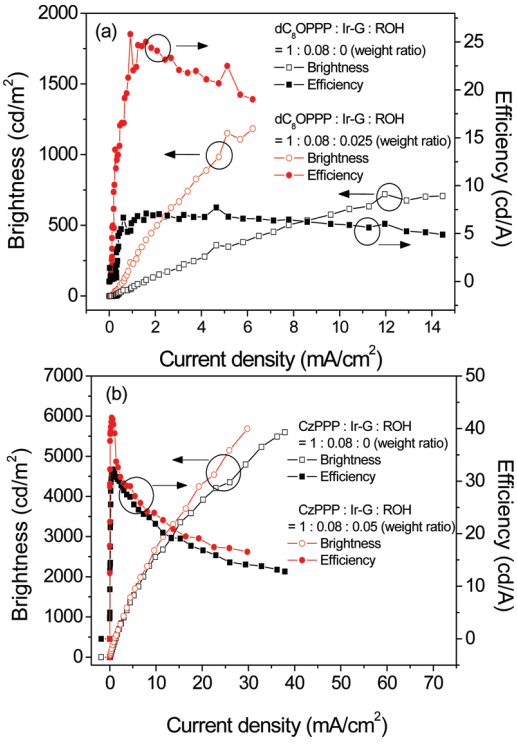

FIGURE 2. Luminous efficiency and brightness versus current density for Ir-G doped (a) dC_8OPPP and (b) CzPPP devices with and without the addition of ROH. The weight ratios of Ir-G and ROH are relative to host polymer.

is ascribed to the increased separation between the polymer and Ir-G by the insertion of ROH between them possibly through a formation of hydrogen bonding of ROH with the dopant and polymer as both containing electron donating sites: C—O—C and N in the amine of the polymer and N in the pyridine ring and C═O in the ligand of the dopant. As a result, the shielding of triplet energy back transfer from the Ir-G to the polymer is further enhanced in addition to that provided by the dense side chains in the polymers. However, as can be seen in Table 1, the mole ratio of ROH to dC_8OPPP repeat unit is 0.041 (which is very close to that of Ir-G (0.044)) at the best device performance condition, which is too small to significantly enhance the shielding effect for dC_8OPPP. Therefore, the possible reason for this optimal efficiency is due to enhanced shielding of Ir-G. In the case of CzPPP/Ir-G, the best device efficiency condition is not at the mole ratio of ROH to Ir-G at 1 but at the mole ratio of 1.9, indicating that the high basicity N atoms on Cz moiety also participate the competition of hydrogen bonding with Ir-G. The schematic illustration of the reduction of back triplet energy tranfer from Ir-G to PPPs is shown in Figure 3.

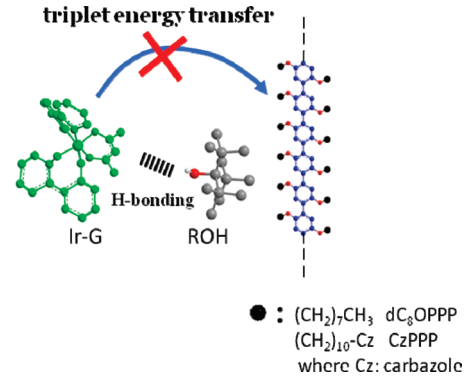

FIGURE 3. Schematic illustration of reduction of back triplet energy tranfer from Ir-G to PPPs. The formation of self-assembly structure between ROH and Ir-G via hydrogen bonding can significantly reduce close contact between main chain of PPPs and Ir-G and therefore minimize back triplet energy transfer from Ir-G to PPPs.

To demonstrate the formation of hydrogen bonding, we have performed FTIR measurements on dC_8OPPP/ROH (1:2 mol ratio), CzPPP/ROH (1:4 mol ratio), and Ir-G/ROH (1:4 mol ratio) films (the mole of each polymer is calculated based on its repeat unit). However, as shown in Figure S1 in the Supporting Information, we found that there is no apparent shift in absorption wavenumbers of the characteristic aliphatic C—O, aliphatic C—N (and aliphatic C—O), and C═N (and C═O) groups for dC_8OPPP, CzPPP, and Ir-G, respectively, which are possible sites for forming hydrogen bonding with O—H group of ROH. [FTIR absorption wavenumbers of the fuctional groups are 1211 cm^{-1} for aliphatic C—O of dC_8OPPP; 1330 and 1221 cm^{-1} for aliphatic C—N and C—O of CzPPP, respectively; 1605 and 1579 cm^{-1} for C═O and C═N of Ir-G.] The observation of no obvious shift in absorption wavenumbers for the functional groups able to form hydrogen bonding with ROH also happens to the three components blends, dC_8OPPP/Ir-G/ROH (1:0.044:0.041 mol ratio) and CzPPP/Ir-G/ROH (1:0.096:0.18 mol ratio) films (see Figure S2 in the Supporting Information), which are the optimum compositions to obtain the best device performance for each host polymer. In general, the formation of hydrogen bonding between linear alcohol and electron-rich functional groups can cause obvious absorption wavenumber shifts of the latter. For example, there is a 31 cm^{-1} red-shift for the C═O stretching mode while acetone

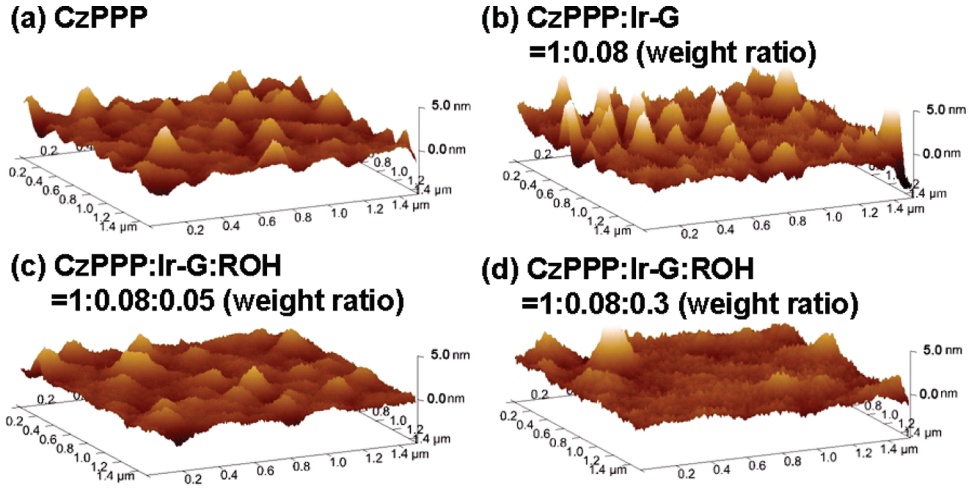

FIGURE 4. Topographical images of the four samples: (a) CzPPP, (b) CzPPP/Ir-G (1:0.08 weight ratio), (c) CzPPP/Ir-G/ROH (1:0.08:0.05 weight ratio), and (d) CzPPP/Ir-G/ROH (1:0.08:0.3 weight ratio), as measured by a scanning probe microscope using tapping mode.

is mixed with ethanol (17), and a 20 cm^{-1} red-shift can be observed for C−O streching mode of the ether group while poly(2-methoxyethyl vinyl ether) is in water (18). Therefore, our FTIR results indicate that hydrogen bonding might occur but is too weak to be detected by FTIR, which may be due to the bulky alkyl group in ROH that makes it difficult to maintain hydrogen bonding in the film state.

In spite of no direct evidence of hydrogen-bonding formation from the absorption wavenumber shift of the corresponding functional group in the FTIR measurement, morphological investigation could give an indirect evidence for the interactions of the added branched alcohol with the polymer and phosphor and thus additional shielding effect in our systems. The topographical images of pristine and blended polymer films for CzPPP are shown in Figure 4. Figure 4a shows that CzPPP has a rather smooth surface with bumps having the average height 0.855 nm. Upon doping with Ir-G into the polymer host (weight ratio 0.08:1), only little phase separation occurs between the dopant and polymer as the average height of the bumps increases slightly from 0.855 to 1.20 nm (Figure 4b). When ROH (weight ratio 0.05 relative to CzPPP) is added into CzPPP/Ir-G, the extent of phase separation is reduced as reflected in the decreased average height of the bumps 0.77 nm, smaller than those of CzPPP and CzPPP/Ir-G (Figure 4c). When the weight ratio of ROH relative to CzPPP increases to 0.3, the average height of bumps is further reduced (0.672 nm, the highest bump in the left part of Figure 4d was not taken in the calculation). It seems that ROH serves as a compatibizer between the dopant and polymer, which might be due to the interaction between ROH with CzPPP and Ir-G (possibly through hydrogen bonding) that prevents Ir-G from aggregation and thus reduces the extent of phase separation in the blended system.

CONCLUSIONS

In summary, we demonstrate that the addition of ROH into dC_8OPPP and CzPPP can further reduce the possible contact between the main chains of these two PPPs and Ir-G by formation of self-assembly structure between ROH and Ir-G possibly via hydrogen bonding, which leads to an enhancement of shielding of triplet energy transfer to PPPs from the phosphor Ir-G, and therefore promote efficiency of electrophosphorescent LEDs. With the addition of appropriate amounts of ROH in the emitting layer (dC_8OPPP/Ir-G and CzPPP/Ir-G), the corresponding device performance can be improved from 7.1 and 32.2 cd/A to 25.1 and 42 cd/A, respectively. The latter result, 42 cd/A, is the highest record in device performance of PLED.

Acknowledgment. This research was supported by the Ministry of Education (Project NSC96-2752-E-007-008-PAE) and the National Science council (Project NSC94-2216-E-007-034, NSC95-2221-E-007-085, and NSC96-2221-E-007-021).

Supporting Information Available: FTIR experimental results for two-component blends (dC_8OPPP/ROH (1:2 mol ratio), CzPPP/ROH (1:4 mol ratio), and Ir-G/ROH (1:4 mol ratio)) and three-component blends (dC_8OPPP/Ir-G/ROH (1:0.044:0.041 mol ratio) and CzPPP/Ir-G/ROH (1:0.096:0.18 mol ratio)) films (PDF). This material is available free of charge via the Internet at http://pubs.acs.org.

REFERENCES AND NOTES

(1) Baldo, M. A.; O'Brien, D. F.; Thompson, M. E.; Forrest, S. R. *Phys. Rev. B* **1999**, *60*, 14422–14428.
(2) Segal, M.; Baldo, M. A.; Holmes, R. J.; Forrest, S. R.; Soos, Z. G. *Phys. Rev. B* **2003**, *68*, 075211/1–075211/14.
(3) Rothe, C.; King, S. M.; Monkman, A. P. *Phys. Rev. Lett.* **2006**, *97*, 076602/1–076602/4.
(4) Baldo, M. A.; O'Brien, D. F.; You, Y.; Shoustikov, A.; Sibley, S.; Thompson, M. E.; Forrest, S. R. *Nature* **1998**, *395*, 151–154.
(5) Tang, K.-C.; Liu, K.-L.; Chen, I.-C. *Chem. Phys. Lett.* **2004**, *386*, 437–441.
(6) Baldo, M. A.; Forrest, S. R. *Phys. Rev. B* **2000**, *62*, 10958–10966.
(7) Sudhakar, M.; Djurovich, P. I.; Hogen-Esch, T. E.; Thompson, M. E. *J. Am. Chem. Soc.* **2003**, *125*, 7796–7797.
(8) Van Dijken, A.; Bastiaansen, J.; Kiggen, N. M. M.; Langeveld, B. M. W.; Rothe, C.; Monkman, A.; Bach, I.; Stossel, P.; Brunner, K. *J. Am. Chem. Soc.* **2004**, *126*, 7718–7727.
(9) Chen, Y.-C.; Huang, G.-S.; Hsiao, C.-C.; Chen, S.-A. *J. Am. Chem. Soc.* **2006**, *128*, 8549–8558.

(10) Hertel, D.; Setayesh, S.; Nothofer, H. G.; Scherf, U.; Müllen, K.; Bässler, H. *Adv. Mater.* **2001**, *13*, 65–70.
(11) Turro, N. J. *Modern Molecular Photochemistry*; University Science Books: Sausalito, CA, 1991; p 328.
(12) Evans, N. R.; Devi, L. S.; Mak, C. S. K.; Watkins, S. E.; Pascu, S. I.; Köhler, A.; Friend, R. H.; Williams, C. K.; Holmes, A. B. *J. Am. Chem. Soc.* **2006**, *128*, 6647–6656.
(13) King, S. M.; Al-Attar, H. A.; Evans, R. J.; Congreve, A.; Beeby, A.; Monkman, A. P. *Adv. Funct. Mater.* **2006**, *16*, 1043–1050.
(14) Huang, S.-P.; Jen, T.-H.; Chen, Y.-C.; Hsiao, A.-E.; Yin, S.-H.; Chen, H.-Y.; Chen, S.-A. *J. Am. Chem. Soc.* **2008**, *130*, 4699–4707.
(15) Hsiao, C.-C.; Chang, C.-H.; Jen, T.-H.; Hung, M.-C.; Chen, S.-A. *Appl. Phys. Lett.* **2006**, *88*, 033512/1–033512/3.
(16) Hsiao, C.-C.; Chang, C.-H.; Lu, H.-H.; Chen, S.-A. *Org. Electron.* **2007**, *8*, 343–348.
(17) Pimentel, G. C.; McClellan, A. L. *The Hydrogen Bond*; W.H. Freeman: San Francisco, 1960; p 137.
(18) Maeda, Y.; Yamauchi, H.; Fujisawa, M.; Sugihara, S.; Ikeda, I. *Langmuir* **2007**, *23*, 6561–6566.

AM900878F